PRAMANA
— journal of
physics

© Printed in India

Vol. 41, No. 4,
October 1993
pp. 371–388

Electron impact excitation of Ni XIX using the *R*-matrix method

MAN MOHAN*, M LE DOURNEUF†, A HIBBERT‡ and V M BURKE‡
*Department of Physics and Astrophysics, Delhi University, Delhi 110007, India
†Laboratoire de Théorie des Processus Atomiques et Moléculaires (U.P.R. 261 du C.N.R.S.), Départment "Atomes et Molécules en Astrophysique", Observatoire de Paris, 92195 Meudon, France
‡Department of Applied Mathematics and Theoretical Physics, The Queen's University, Belfast BT7 1NN, UK

MS received 12 July 1993

Abstract. Collision strengths for all the transitions between the 15 lowest states of neon-like Ni XIX have been calculated for electron impact in the 80–140 Ry energy range. Configuration-interaction wavefunctions have been used to represent the target states. The standard *R*-matrix code has been used to calculate the lower scattering partial waves ($L \leqslant 9$), while a no-exchange version of the same code has been used to compute efficiently the higher partial waves ($L \geqslant 10$). Effective collision strengths for 105 excitation transitions between the ground state $2s^2 2p^6\,{}^1S^e$ and the 14 $2s^2 2p^5 3l$ Rydberg states are tabulated for electron temperatures in the range $\log T = 5{\cdot}40$ to $\log T = 7{\cdot}00$, with T expressed in °K.

Keywords. Collision strength; configuration interaction.

PACS No. 34·80

1. Introduction

The interaction of electrons and photons with ionized atoms, particularly with metallic impurities such as Ti, Cr, Fe and Ni, plays an important role in fusion plasmas, as discussed in the recent meeting of the International Atomic Energy Agency [1]. Data on these processes are required both for plasma diagnostics and in plasma modelling. They are also required in laser research, especially in the soft X-ray region where Ne-like ions play a specific role in the electron excitation scheme as illustrated by the recent work of Matthews *et al* [2].

The first line of identifications for Ni XIX were made by Feldman *et al* [3], who reported transitions from the $2p^5 3s$, $2p^5 3d$ and $2s2p^6 3p$ configurations. A complete line classification, usable for the identification of solar features, was then undertaken by Swartz *et al* [4]. By analysing the soft X-ray spectra from 8 to 18 Å for the ions of Cr, Mn, Fe, Co, Ni and Cu, they identified lines originating from the $2p^5 4s$, $2p^5 5d$ and $2p^5 6d$ configurations.

Several theoreticians have reported calculations of atomic data for the Ne-like ions. Bhatia *et al* [5] have used the distorted wave approximation to compute collision strengths for the transitions from the ground level to the $n = 3$ Ry levels of the Ne-like ions with nuclear charge $Z = 14$, 18, 22, 26, 32 and 36. Zhang *et al* have reported collision strengths for excitation from the ground to the $n = 3$ and $n = 4$ levels in 20 neon-like ions with nuclear charge Z in the range $18 \leqslant Z \leqslant 74$, using the Coulomb–Born (1987) and relativistic distorted wave (1989) methods. Hagelstein and Jung [6] have also used a relativistic distorted wave, method to obtain collision strengths for neon-like ions with $Z = 26$, 34, 39, 42 and 47.

In the present work, we have used the R-matrix method [7], which allows the explicit introduction of the effect of resonances converging on to all the excited target terms included in the calculation. We have performed a 15-state calculation in LS coupling. The 15 target states $2s^2 2p^6 (^1S^e)$, $2s^2 2p^5 3s(^{1,3}P^0)$, $2s^2 2p^5 3p(^{1,3}S^e$, $^{1,3}P^e$, $^{1,3}D^e)$, $2s^2 2p^5 3d(^{1,3}P^0$, $^{1,3}D^0$, $^{1,3}F^0)$ are represented by configuration interaction wavefunctions. The effective collision strengths, obtained by averaging the collision strengths over a Maxwellian distribution for the velocity of the incident electron, are tabulated over a wide range of temperatures.

We have used the standard R-matrix code of Berrington *et al* [8, 9] for low partial waves ($L \leqslant 9$) and the no-exchange R-matrix program recently developed by Burke *et al* [10] for partial waves $10 \leqslant L \leqslant 40$. In addition, for optically allowed transitions, a 'top up' procedure based on the sum rule of Burgess *et al* [11] has been used to account approximately for $L > 40$.

2. Target calculation

Using the general configuration interaction (CI) code CIV3 [12], Hibbert *et al* [13] have calculated CI wavefunctions for all the states of the $[1s^2]$ $2s^2 2p^6$, $2s^2 2p^5 3l$, $2s 2p^6 3l (l = s, p, d)$ configurations of many ions of the neon isoelectronic sequence, including Ni XIX. In the present scattering calculation, the fifteen lowest ionic states belonging to the ground $2s^2 2p^6$ and the $n = 3$ Rydberg $2s^2 2p^5 3l (l = s, p, d)$ configurations are represented by restricted CI expansions, which include the most important configurations while keeping the scattering calculation tractable.

The wavefunctions are represented by expansions of the form

$$\Phi(LS) = \sum_{i=1}^{M} a_i \phi_i(\alpha_i, LS), \tag{1}$$

where the single configuration functions ϕ_i are constructed from one electron orbitals, whose angular momenta are coupled as specified by α_i to form total L and S common to the M configurations. The radial part of each orbital is written as a linear combination of normalized Slater-type orbitals:

$$P_{nl} = \sum_{i=1}^{k} b_i \left[\frac{(2\zeta_i)^{2p_i + 1}}{(2p_i)!} \right]^{1/2} r^{p_i} \exp(-\zeta_i r) \tag{2}$$

The parameters b_i, ζ_i in eq (2) and the mixing coefficients a_i in (1) are determined variationally as described by Hibbert *et al* [13].

In order to represent in a balanced way the ground and all the $n = 3$ Ry states, we used eight orthogonal one-electron orbitals $1s$, $2s$, $2p$, $3s$, $3p$, $4p$, $3d$, $4d$. The $1s$, $2s$ and $2p$ orbitals were initially chosen as the Hartree–Fock orbitals for the ground $^2P^0$ state of the fluorine-like Ni XX ion [14], with the $1s$ and $2s$ functions kept frozen throughout the calculation. The $3s$ function was first optimized on the energy of the lowest $2p^5 3s\, ^3P^0$ Rydberg state of Ni XIX. The $2p$ was then reoptimized on the same state. Since the new $2p$ function is not the best one to represent the $2s^2 2p^6\, ^1S^e$ ground state, we introduced a $3p$ function to compensate for this, optimising its parameters by minimizing the lowest energy eigenvalue in the $(2s^2 2p^6 + 2s^2 2p^5 3p)$ $^1S^e$ subspace. This $3p$ function then provided some flexibility to represent the '$2p$' orbitals optimal for the different target states. The $4p$ orbital was optimized on the lowest eigenvalue in the $(2p^5 3p + 2p^5 4p)$ $^3S^e$ subspace. The $3d$ function was chosen to optimize the lowest energy eigenvalue arising from the configurations $(2s^2 2p^5 3s + 2s3d2p^5 3s)$ $^3P^0$, in order to account for the important $s-d$ angular correlation. Finally, the $4d$ orbital was optimized by minimizing the lowest eigenvalue in the subspace $(2p^5 3d + 2p^5 4d)$ $^3D^0$.

In table 1, we present our optimized parameters b_i, p_i and ζ_i for the $3s$, $2p$, $3p$, $4p$, $3d$ and $4d$ orbitals. Table 2 gives the restricted list of configurations included in the scattering calculation to represent the 15 target states, which are indexed in order of

Table 1. Values of parameters b_i, p_i and ξ_i for bound orbitals of Ni XIX.

Orbital	Clementi coefficient b_i	Power of r p_i	Exponent ζ_i
$3s$	0·23125	1	20·60692
	−1·12640	2	8·98607
	1·60027	3	6·92923
$2p$	0·33249	2	12·46111
	0·09747	2	19·34179
	0·58600	2	10·93709
$3p$	2·38031	2	9·83896
	−2·76992	3	10·38145
$4p$	1·78688	2	10·37242
	−3·15633	3	10·10618
	2·01926	4	7·75928
$3d$	1·00000	3	13·18651
$4d$	0·63329	3	14·11282
	−1·14731	4	7·81852

Table 2. Configurations used in the CI expansion of Ni XIX target states.

Target states	State Number	Configuration used
$^1S^e$	1, 9	$[1s^2]2s^2 2p^6, 2s^2 2p^5 3p, 2s^2 2p^5 4p, 2s2p^6 3s$
$^3P^0$	2, 10	$[1s^2]2s^2 2p^5 3s, 2s^2 2p^5 3d, 2s^2 2p^5 4d,$ $2s2p^6 3p, 2s2p^6 4p$
$^1P^0$	3, 15	$[1s^2]2s^2 2p^5 3s, 2s^2 2p^5 3d, 2s^2 2p^5 4d,$ $2s2p^6 3p, 2s2p^6 4p$
$^3S^e$	4	$[1s^2]2s^2 2p^5 3p, 2s^2 2p^5 4p, 2s2p^6 3s$
$^3D^e$	5	$[1s^2]2s^2 2p^5 3p, 2s^2 2p^5 4p, 2s2p^6 3d, 2s2p^6 4d$
$^1D^e$	6	$[1s^2]2s^2 2p^5 3p, 2s^2 2p^5 4p, 2s2p^6 3d, 2s2p^6 4d$
$^3P^e$	7	$[1s^2]2s^2 2p^5 3p, 2s^2 2p^5 4p$
$^1P^e$	8	$[1s^2]2s^2 2p^5 3p, 2s^2 2p^5 4p$
$^3F^0$	11	$[1s^2]2s^2 2p^5 3d, 2s^2 2p^5 4d$
$^1F^0$	12	$[1s^2]2s^2 2p^5 3d, 2s^2 2p^5 4d$
$^3D^0$	13	$[1s^2]2s^2 2p^5 3d, 2s^2 2p^5 4d$
$^1D^0$	14	$[1s^2]2s^2 2p^5 3d, 2s^2 2p^5 4d$

Table 3. Excitation thresholds for Ni XIX (in Ryd.).

Key	Configuration	State	Theory	Experiment
1	$1s^2 2s^2 2p^6$	$^1S^e$	0·00000	0·00000
2	$1s^2 2s^2 2p^5 3s$	$^3P^0$	65·14602	64·80838
3	$1s^2 2s^2 2p^5 3s$	$^1P^0$	65·40276	66·18554
4	$1s^2 2s^2 2p^5 3p$	$^3S^e$	67·30349	
5	$1s^2 2s^2 2p^5 3p$	$^3D^e$	67·77201	
6	$1s^2 2s^2 2p^5 3p$	$^1D^e$	67·98450	
7	$1s^2 2s^2 2p^5 3p$	$^3P^e$	68·03022	
8	$1s^2 2s^2 2p^5 3p$	$^1P^e$	68·03022	
9	$1s^2 2s^2 2p^5 3p$	$^1S^e$	69·74102	
10	$1s^2 2s^2 2p^5 3d$	$^3P^0$	71·07860	71·19752
11	$1s^2 2s^2 2p^5 3d$	$^3F^0$	71·30784	
12	$1s^2 2s^2 2p^5 3d$	$^1F^0$	71·56094	
13	$1s^2 2s^2 2p^5 3d$	$^3D^0$	71·64446	72·04501
14	$1s^2 2s^2 2p^5 3d$	$^1D^0$	71·64446	
15	$1s^2 2s^2 2p^5 3d$	$^1P^0$	72·61951	73·37546

increasing energy. Table 3 shows that the excitation thresholds, calculated with these fairly simple wavefunctions, agree reasonably well with the experimental results of Corliss and Sugar [15].

3. Scattering calculation

In an inner region $r < a$ containing the charge distribution of the N-electron target, the total wavefunction describing the $(N+1)$-electron system is expanded on a discrete basis of R-matrix states [16, 8]:

$$\Psi_k = \mathscr{A} \sum_{ij} c_{ijk} \Phi_i(x_1 \cdots x_N, \hat{\mathbf{r}}_{N+1}, \sigma_{N+1}) u_{ij}(r_{N+1}) + \sum_j d_{jk} \phi_j(x_1 \cdots x_{N+1}), \quad (3)$$

where $\mathscr{A}$ is the antisymmetrization operator which accounts for electron exchange, Φ_i are channel functions formed by coupling the target states of coordinates $x_i = \{r_i, \hat{\mathbf{r}}_i, \sigma_i\}$ with the spin angle function of the scattered electron. The $\{u_{ij}\}$ form a discrete R-matrix basis of continuum orbitals for the scattered electron and the $\{\phi_j\}$ are $(N+1)$ electron bound configurations, which account for the orthogonality of the continuum orbitals u_{ij} to the bound orbitals and for additional short range correlation effects.

The continuum orbitals u_{ij} in (3) are solutions of the zero-order radial differential equation:

$$\left[-\frac{d^2}{dr^2} + \frac{l_i(l_i+1)}{r^2} + 2V(r) - k_i^2 \right] u_{ij}(r) = \sum_k \lambda_{ijk} P_k(r), \quad (4)$$

which satisfy the boundary conditions:

$$u_{ij}(0) = 0 \quad (5a)$$

$$\frac{a}{u_{ij}} \frac{du_{ij}}{dr}\bigg|_{r=a} = b. \quad (5b)$$

In (4), l_i is the angular momentum of the scattered electron, $V(r)$ is the static potential of the target in its ground state and λ_{ijk} are Lagrange multipliers which are determined in order to ensure the orthogonality of the continuum orbitals to the bound radial orbitals $P_{kl_i}(r)$ having the same angular momentum l_i. We imposed a zero logarithmic derivative $b=0$ at the R-matrix boundary radius $a=3{\cdot}5$ a.u. and we retained 20 continuum orbitals for each angular symmetry, to ensure convergence in the energy range considered here, namely up to 172 Ryd.

The coefficients c_{ijk} and d_{jk} in (3) were determined by diagonalizing the $(N+1)$-electron Hamiltonian matrix in the inner region. In the outer region ($r \geqslant a$), the radial equations were solved, using the asymptotic code of Berrington *et al* [9] which treats multipole couplings by first order perturbation theory [17]. The LS coupled K matrices, obtained by matching the inner and outer solutions at the R-matrix boundary, were used to calculate collision strengths. We have considered all partial waves, up to $L=9$ for both parities and spin multiplicities (doublet and quartet). This was sufficient to obtain converged results for forbidden transitions from the ground state $^1S^e$. However, for dipole allowed transitions, such as $2p^6\,{}^1S^e \rightarrow 3s\,{}^1P^0$, it was necessary to include the contribution of higher partial waves for convergence. Since exchange effects were found to be negligible for $L \geqslant 10$, a no-exchange R-matrix approximation, which amounts to neglecting the antisymmetrization and the bound-type part of expansion (3), is sufficient for higher partial waves. A fast no-exchange R-matrix code, recently developed by Burke *et al* [10], has therefore been used to calculate the contributions from $L=10$ to 40 and, finally, a 'top up' procedure, based on the sum rule of Burgess *et al* [11], accounts approximately for $L>40$.

Another important aspect of the calculation is that, above all thresholds, the pseudo-resonances, induced in the low partial waves by some bound-type terms in expansion (3), have been removed by smoothing the T-matrix according to the method of Burke *et al* [16].

4. Results and discussion

The importance of the smoothing procedure on the collision strengths is illustrated in figure 1 and table 4 which compare the raw Ω_{EX} and the smoothed $\bar{\Omega}_{\mathrm{EX}}$ contributions of the $L \leqslant 9$ partial waves, including exchange, for the $2p^5\,3p\,{}^3S^e \rightarrow {}^3D^e$ transition from 85 to 160 Rydberg. Table 4 also illustrates the importance of the no-exchange contributions Ω_{NE} obtained by the no-exchange code for $10 \leqslant L \leqslant 40$ and the 'top up' procedure for $L>40$. Indeed, for the ${}^3S^e \rightarrow {}^3D^e$ transition, the $L \geqslant 10$ partial waves contribute from 6% to 14% of the total collision strength when the energy increases from 85 to 100 Ryd.

The present R-matrix (RM) calculation is the first one to give excitation collision strengths between the $n=3$ Rydberg states (table 5). Comparison with the previous relativistic distorted wave (RDW) calculation of Zhang *et al* [18] is therefore limited to the collision strengths for excitation from the ground state. Since the RDW results were obtained at impact energies which are multiples of each threshold excitation energy E_I, a spline interpolation of our RM results has been made to facilitate the comparison. In addition, since our calculation is performed in LS coupling, we limit our comparison in table 6 to transitions involving pure ${}^3P_2^0$ and nearly pure ${}^1S_0^e$ states. For the spin-forbidden transition to the first excited level, $2p^6\,{}^1S_0^e \rightarrow 2p^5\,3s\,{}^3P_2^0$, we notice that the results of the two calculations decrease monotonically at high

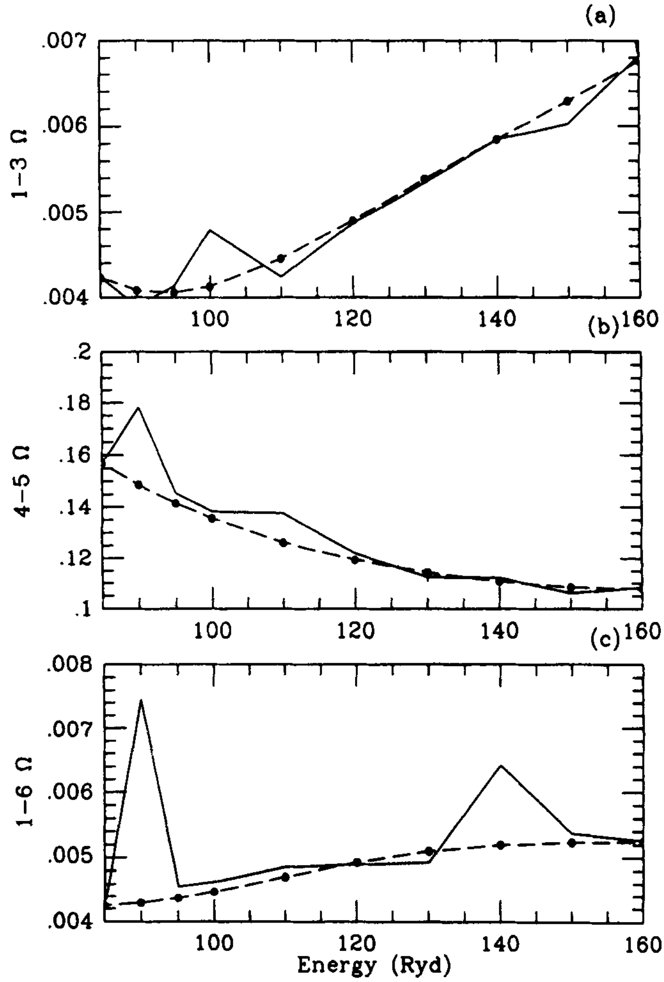

Figure 1. Collision strengths for various transitions as a function of electron energy. Full curves: raw collision strengths, broken curves: collision strengths obtained by averaging over pseudo-resonances.

Table 4. Influence of higher partial waves and of the smoothing of pseudo-resonances on the collision strength for the $2p^5 3p\,^3P^e \rightarrow {}^3D^e$ transition.

Energy in Ryd.	Ω_{EX} $L \leqslant 9$	$\bar{\Omega}_{EX}$ $L \leqslant 9$	Ω_{NE} $10 \leqslant L \leqslant 40$ + 'top up'	Total $\Omega = \bar{\Omega}_{EX} + \Omega_{NE}$
85·00	0·1569	0·1569	0·0128	0·1697
90·00	0·1781	0·1485	0·0151	0·1636
93·00	0·1454	0·1415	0·0172	0·1587
100·00	0·1382	0·1356	0·0194	0·1550

energies, the RDW results are globally smaller and their relative difference decreases from more than 40% at $E/E_I = 1{\cdot}5$ to 28% at $E/E_I = 1{\cdot}9$. For the $2p^6\,^1S_0^e \rightarrow 2p^5 3d\,^3P_2^0$ transition, we observe the same trends, with the relative difference between the two calculations decreasing from 40% at $E/E_I = 1{\cdot}2$ to 27% at $E/E_I = 1{\cdot}9$. In the case of

Table 5. Collision strengths for transitions in Ni XIX in the energy range 80–140 Ryd. ($a \pm b \equiv a \times 10^{\pm b}$).

Transition		Energy (Ryd.)								
i	f	80·00	85·00	90·00	95·00	100·00	110·00	120·00	130·00	140·00
1	2	2·866 − 3	2·903 − 3	2·640 − 3	2·416 − 3	2·225 − 3	1·915 − 3	1·673 − 3	1·473 − 3	1·300 − 3
1	3	3·181 − 3	4·240 − 3	4·101 − 3	4·089 − 3	4·177 − 3	4·564 − 3	5·117 − 3	5·740 − 3	6·371 − 3
1	4	4·346 − 3	4·188 − 3	3·678 − 3	3·263 − 3	2·930 − 3	2·468 − 3	2·224 − 3	2·156 − 3	2·251 − 3
1	5	8·266 − 3	7·852 − 3	6·620 − 3	5·668 − 3	4·943 − 3	4·012 − 3	3·589 − 3	3·585 − 3	4·054 − 3
1	6	4·124 − 3	4·278 − 3	4·338 − 3	4·444 − 3	4·584 − 3	4·925 − 3	5·292 − 3	5·635 − 3	5·932 − 3
1	7	3·204 − 3	3·054 − 3	2·599 − 3	2·235 − 3	1·948 − 3	1·561 − 3	1·370 − 3	1·333 − 3	1·445 − 3
1	8	1·274 − 3	1·218 − 3	1·051 − 3	9·165 − 4	8·071 − 4	6·568 − 4	5·771 − 4	5·539 − 4	5·821 − 4
1	9	3·441 − 2	3·483 − 2	3·202 − 2	3·008 − 2	2·886 − 2	2·824 − 2	2·975 − 2	3·348 − 2	4·001 − 2
1	10	1·564 − 2	1·455 − 2	1·330 − 2	1·223 − 2	1·129 − 2	9·720 − 3	8·453 − 3	7·443 − 3	6·742 − 3
1	11	1·413 − 2	1·306 − 2	1·165 − 2	1·033 − 2	9·332 − 3	7·827 − 3	6·759 − 3	6·042 − 3	5·781 − 3
1	12	3·344 − 3	3·535 − 3	3·532 − 3	3·585 − 3	3·679 − 3	3·942 − 3	4·246 − 3	4·547 − 3	4·845 − 3
1	13	5·641 − 3	5·133 − 3	4·496 − 3	3·981 − 3	3·562 − 3	2·918 − 3	2·445 − 3	2·103 − 3	1·940 − 3
1	14	1·958 − 3	1·745 − 3	1·568 − 3	1·420 − 3	1·297 − 3	1·100 − 3	9·492 − 4	8·351 − 4	7·655 − 4
1	15	5·564 − 2	5·495 − 2	5·429 − 2	5·390 − 2	5·356 − 2	5·342 − 2	5·349 − 2	5·359 − 2	5·347 − 2
2	3	9·945 − 2	1·055 − 1	1·095 − 1	1·140 − 1	1·186 − 1	1·285 − 1	1·387 − 1	1·491 − 1	1·591 − 1
2	4	4·852 − 2	4·495 − 2	4·188 − 2	3·922 − 2	3·478 − 2	3·113 − 2	2·807 − 2	2·562 − 2	2·411 − 2
2	5	1·546 − 0	1·625 − 0	1·690 − 0	1·753 − 0	1·828 − 0	1·915 − 0	1·960 − 0	2·013 − 0	2·067 − 0
2	6	8·664 − 0	9·015 − 0	9·360 − 0	9·629 − 0	1·001 + 1	1·047 + 1	1·073 + 1	1·102 + 1	1·130 + 1
2	7	1·081 − 2	9·386 − 3	8·197 − 3	7·210 − 3	5·712 − 3	4·668 − 3	3·908 − 3	3·308 − 3	2·799 − 3
2	8	5·147 − 0	5·340 − 0	5·590 − 0	5·760 − 0	6·004 − 0	6·276 − 0	6·464 − 0	6·653 − 0	6·831 − 0
2	9	6·534 − 3	5·674 − 3	4·957 − 3	4·362 − 3	3·463 − 3	2·841 − 3	2·392 − 3	2·044 − 3	1·752 − 3
2	10	2·209 − 3	1·922 − 3	1·683 − 3	1·487 − 3	1·189 − 3	9·804 − 4	8·248 − 4	6·974 − 4	5·854 − 4
2	11	2·229 − 1	2·465 − 1	2·838 − 1	3·213 − 1	3·581 − 1	3·254 − 1	2·548 − 1	2·466 − 1	4·656 − 1
2	12	5·110 − 1	5·130 − 1	5·155 − 1	5·187 − 1	5·242 − 1	5·301 − 1	5·319 − 1	5·311 − 1	5·279 − 1
2	13	1·599 − 2	1·378 − 2	1·194 − 2	1·041 − 2	8·086 − 3	6·473 − 3	5·329 − 3	4·507 − 3	3·952 − 3
2	14	3·541 − 1	3·527 − 1	3·549 − 1	3·567 − 1	3·609 − 1	3·651 − 1	3·679 − 1	3·711 − 1	3·784 − 1
2	15	1·135 − 2	9·743 − 3	8·457 − 3	7·416 − 3	5·836 − 3	4·665 − 3	3·778 − 3	3·268 − 3	3·440 − 3

(*Continued*)

Table 5. *(Continued)*

Transition		Energy (Ryd.)								
i	*f*	80·00	85·00	90·00	95·00	100·00	110·00	120·00	130·00	140·00
3	4	7·547 − 3	6·520 − 3	5·654 − 3	4·927 − 3	3·811 − 3	3·029 − 3	2·471 − 3	2·056 − 3	1·737 − 3
3	5	2·044 − 3	1·774 − 3	1·552 − 3	1·371 − 3	1·102 − 3	9·186 − 4	7·848 − 4	6·773 − 4	5·850 − 4
3	6	1·078 − 2	9·475 − 3	8·375 − 3	7·449 − 3	6·009 − 3	4·960 − 3	4·153 − 3	3·486 − 3	2·896 − 3
3	7	2·950 − 0	3·070 − 0	3·190 − 0	3·284 − 0	3·441 − 0	3·549 − 0	3·662 − 0	3·785 − 0	3·858 − 0
3	8	6·328 − 3	5·492 − 3	4·799 − 3	4·227 − 3	3·366 − 3	2·769 − 3	2·333 − 3	1·988 − 3	1·697 − 3
3	9	1·692 − 0	1·759 − 0	1·842 − 0	1·898 − 0	1·988 − 0	2·061 − 0	2·130 − 0	2·199 − 0	2·249 − 0
3	10	5·253 − 1	5·497 − 1	5·732 − 1	5·933 − 1	6·284 − 1	6·522 − 1	6·817 − 1	7·119 − 1	7·290 − 1
3	11	7·071 − 3	5·944 − 3	5·094 − 3	4·443 − 3	3·505 − 3	2·813 − 3	2·291 − 3	2·106 − 3	2·663 − 3
3	12	1·591 − 2	1·357 − 2	1·169 − 2	1·019 − 2	7·972 − 3	6·436 − 3	5·295 − 3	4·477 − 3	4·120 − 3
3	13	1·603 − 1	1·615 − 1	1·628 − 1	1·644 − 1	1·675 − 1	1·706 − 1	1·733 − 1	1·756 − 1	1·765 − 1
3	14	1·089 − 2	9·516 − 3	8·374 − 3	7·417 − 3	5·907 − 3	4·755 − 3	3·843 − 3	3·167 − 3	2·833 − 3
3	15	1·087 − 1	1·092 − 1	1·105 − 1	1·115 − 1	1·135 − 1	1·155 − 1	1·171 − 1	1·182 − 1	1·186 − 1
4	5	7·271 − 2	7·365 − 2	7·451 − 2	7·554 − 2	7·776 − 2	7·973 − 2	8·159 − 2	8·312 − 2	8·390 − 2
4	6	1·697 − 1	1·637 − 1	1·588 − 1	1·550 − 1	1·497 − 1	1·469 − 1	1·455 − 1	1·456 − 1	1·467 − 1
4	7	6·509 − 3	5·885 − 3	5·386 − 3	4·986 − 3	4·392 − 3	3·976 − 3	3·686 − 3	3·548 − 3	3·664 − 3
4	8	1·753 − 2	1·555 − 2	1·387 − 2	1·247 − 2	1·033 − 2	9·022 − 3	8·275 − 3	8·138 − 3	8·642 − 3
4	9	2·180 − 3	1·929 − 3	1·731 − 3	1·574 − 3	1·349 − 3	1·199 − 3	1·101 − 3	1·059 − 3	1·110 − 3
4	10	3·944 − 3	3·579 − 3	3·274 − 3	3·021 − 3	2·649 − 3	2·416 − 3	2·286 − 3	2·232 − 3	2·238 − 3
4	11	2·187 − 0	2·287 − 0	2·373 − 0	2·446 − 0	2·540 − 0	2·671 − 0	2·749 − 0	2·840 − 0	2·934 − 0
4	12	3·066 − 2	2·961 − 2	2·895 − 2	2·861 − 2	2·856 − 2	2·902 − 2	2·965 − 2	3·025 − 2	3·073 − 2
4	13	6·007 − 3	5·115 − 3	4·385 − 3	3·788 − 3	2·907 − 3	2·316 − 3	1·907 − 3	1·618 − 3	1·434 − 3
4	14	4·420 − 3	3·812 − 3	3·292 − 3	2·850 − 3	2·143 − 3	1·609 − 3	1·200 − 3	8·994 − 4	7·223 − 4
4	15	1·453 − 3	1·110 − 3	8·501 − 4	6·561 − 4	4·136 − 4	2·978 − 4	2·567 − 4	2·711 − 4	3·551 − 4
5	6	5·272 − 3	4·446 − 3	3·789 − 3	3·268 − 3	2·525 − 3	2·041 − 3	1·704 − 3	1·467 − 3	1·345 − 3
5	7	5·880 − 2	5·262 − 2	4·760 − 2	4·354 − 2	3·757 − 2	3·362 − 2	3·101 − 2	2·953 − 2	2·941 − 2
5	8	7·653 − 1	7·482 − 1	7·382 − 1	7·289 − 1	7·163 − 1	7·094 − 1	7·074 − 1	7·075 − 1	7·104 − 1

5	9	4·972 − 2	4·450 − 2	4·009 − 2	3·638 − 2	3·065 − 2	2·670 − 2	2·416 − 2	2·290 − 2	2·304 − 2
5	10	6·474 − 3	5·992 − 3	5·595 − 3	5·264 − 3	4·741 − 3	4·326 − 3	3·955 − 3	3·595 − 3	3·252 − 3
5	11	9·337 − 2	9·238 − 2	9·227 − 2	9·250 − 2	9·347 − 2	9·626 − 2	9·847 − 2	1·010 − 1	1·038 − 1
5	12	9·822 − 0	1·026 + 1	1·071 + 1	1·105 + 1	1·147 + 1	1·206 + 1	1·239 + 1	1·275 + 1	1·310 + 1
5	13	3·292 − 2	2·826 − 2	2·439 − 2	2·120 − 2	1·640 − 2	1·315 − 2	1·090 − 2	9·306 − 3	8·207 − 3
5	14	1·848 − 0	1·914 − 0	2·006 − 0	2·069 − 0	2·152 − 0	2·253 − 0	2·332 − 0	2·405 − 0	2·474 − 0
5	15	1·744 − 2	1·480 − 2	1·263 − 2	1·087 − 2	8·281 − 3	6·577 − 3	5·429 − 3	4·645 − 3	4·171 − 3
6	7	1·155 − 2	9·458 − 3	7·855 − 3	6·636 − 3	5·008 − 3	4·033 − 3	3·401 − 3	3·032 − 3	3·080 − 3
6	8	4·979 − 2	4·419 − 2	3·950 − 2	3·558 − 2	2·965 − 2	2·572 − 2	2·340 − 2	2·255 − 2	2·333 − 2
6	9	2·404 − 1	2·379 − 1	2·371 − 1	2·361 − 1	2·339 − 1	2·321 − 1	2·293 − 1	2·257 − 1	2·222 − 1
6	10	4·267 − 2	4·236 − 2	4·218 − 2	4·211 − 2	4·217 − 2	4·239 − 2	4·267 − 2	4·293 − 2	4·304 − 2
6	11	1·097 − 2	9·411 − 3	8·134 − 3	7·083 − 3	5·490 − 3	4·354 − 3	3·499 − 3	2·853 − 3	2·444 − 3
6	12	3·239 − 2	2·716 − 2	2·296 − 2	1·960 − 2	1·482 − 2	1·179 − 2	9·780 − 3	8·390 − 3	7·513 − 3
6	13	3·263 − 0	3·411 − 0	3·566 − 0	3·680 − 0	3·855 − 0	3·998 − 0	4·140 − 0	4·290 − 0	4·382 − 0
6	14	1·748 − 2	1·486 − 2	1·273 − 2	1·099 − 2	8·430 − 3	6·668 − 3	5·384 − 3	4·425 − 3	3·809 − 3
6	15	6·180 − 1	6·420 − 1	6·754 − 1	6·984 − 1	7·314 − 1	7·599 − 1	7·903 − 1	8·187 − 1	8·392 − 1
7	8	1·701 − 2	1·746 − 2	1·802 − 2	1·859 − 2	1·973 − 2	2·073 − 2	2·158 − 2	2·225 − 2	2·262 − 2
7	9	2·319 − 2	2·127 − 2	1·963 − 2	1·822 − 2	1·596 − 2	1·427 − 2	1·302 − 2	1·217 − 2	1·175 − 2
7	10	2·096 − 3	1·884 − 3	1·708 − 3	1·564 − 3	1·347 − 3	1·203 − 3	1·112 − 3	1·066 − 3	1·070 − 3
7	11	1·781 − 0	1·858 − 0	1·944 − 0	2·006 − 0	2·084 − 0	2·191 − 0	2·256 − 0	2·326 − 0	2·393 − 0
7	12	7·381 − 2	7·056 − 2	6·828 − 2	6·675 − 2	6·526 − 2	6·505 − 2	6·538 − 2	6·603 − 2	6·716 − 2
7	13	1·267 − 2	1·073 − 2	9·148 − 3	7·856 − 3	5·957 − 3	4·701 − 3	3·860 − 3	3·309 − 3	3·032 − 3
7	14	5·414 − 0	5·605 − 0	5·900 − 0	6·082 − 0	6·317 − 0	6·612 − 0	6·828 − 0	7·037 − 0	7·230 − 0
7	15	1·828 − 2	1·543 − 2	1·312 − 2	1·127 − 2	8·593 − 3	6·877 − 3	5·750 − 3	4·997 − 3	4·562 − 3
8	9	6·163 − 3	5·103 − 3	4·271 − 3	3·624 − 3	2·727 − 3	2·168 − 3	1·798 − 3	1·560 − 3	1·493 − 3
8	10	1·592 − 3	1·469 − 3	1·363 − 3	1·270 − 3	1·119 − 3	9·954 − 4	9·063 − 4	8·304 − 4	7·463 − 4
8	11	5·479 − 3	4·699 − 3	4·059 − 3	3·533 − 3	2·731 − 3	2·150 − 3	1·696 − 3	1·328 − 3	1·056 − 3
8	12	1·273 − 2	1·095 − 2	9·469 − 3	8·248 − 3	6·403 − 3	5·127 − 3	4·212 − 3	3·533 − 3	3·047 − 3
8	13	1·558 − 2	1·575 − 2	1·604 − 2	1·641 − 2	1·727 − 2	1·816 − 2	1·989 − 2	1·954 − 2	1·997 − 2
8	14	1·810 − 2	1·550 − 2	1·338 − 2	1·155 − 2	9·058 − 3	7·239 − 3	5·883 − 3	4·848 − 3	4·160 − 3
8	15	1·793 − 0	1·858 − 0	1·959 − 0	2·022 − 0	2·108 − 0	2·195 − 0	2·273 − 0	2·346 − 0	2·404 − 0

(*Continued*)

Table 5. (*Continued*)

Transition		Energy (Ryd.)								
i	f	80·00	85·00	90·00	95·00	100·00	110·00	120·00	130·00	140·00
9	10	5·534 − 1	5·784 − 1	6·091 − 1	6·328 − 1	6·699 − 1	6·991 − 1	7·275 − 1	7·577 − 1	7·765 − 1
9	11	5·207 − 3	4·309 − 3	3·607 − 3	3·063 − 3	2·327 − 3	1·899 − 3	1·657 − 3	1·552 − 3	1·615 − 3
9	12	6·155 − 3	5·045 − 3	4·203 − 3	3·565 − 3	2·714 − 3	2·211 − 3	1·901 − 3	1·762 − 3	1·899 − 3
9	13	6·737 − 3	6·985 − 3	7·259 − 3	7·542 − 3	8·098 − 3	8·581 − 3	8·947 − 3	9·183 − 3	9·301 − 3
9	14	1·575 − 3	1·266 − 3	1·027 − 3	8·438 − 4	5·978 − 4	4·546 − 4	3·701 − 4	3·300 − 4	3·501 − 4
9	15	7·645 − 4	6·493 − 4	5·587 − 4	4·870 − 4	3·822 − 4	3·080 − 4	2·530 − 4	2·206 − 4	2·294 − 4
10	11	7·176 − 1	7·571 − 1	7·882 − 1	8·133 − 1	8·542 − 1	8·819 − 1	9·116 − 1	9·457 − 1	9·628 − 1
10	12	1·439 − 1	1·329 − 1	1·236 − 1	1·154 − 1	1·015 − 1	9·014 − 2	8·024 − 2	7·162 − 2	6·462 − 2
10	13	4·850 − 2	4·286 − 2	3·807 − 2	3·402 − 2	2·771 − 2	2·326 − 2	2·011 − 2	1·791 − 2	1·647 − 2
10	14	2·414 − 1	2·248 − 1	2·115 − 1	2·014 − 1	1·876 − 1	1·794 − 1	1·751 − 1	1·771 − 1	1·896 − 1
10	15	2·114 − 2	1·828 − 2	1·594 − 2	1·402 − 2	1·118 − 2	9·291 − 3	8·088 − 3	7·510 − 3	7·696 − 3
11	12	2·495 − 2	2·206 − 2	1·966 − 2	1·768 − 2	1·471 − 2	1·265 − 2	1·115 − 2	9·944 − 3	8·894 − 3
11	13	1·368 − 1	1·214 − 1	1·082 − 1	9·689 − 2	7·892 − 2	6·565 − 2	5·561 − 2	4·771 − 2	4·125 − 2
11	14	5·753 − 1	5·622 − 1	5·528 − 1	5·445 − 1	5·296 − 1	5·148 − 1	4·994 − 1	4·851 − 1	4·770 − 1
11	15	9·852 − 2	8·729 − 2	7·756 − 2	6·916 − 2	5·575 − 2	4·595 − 2	3·887 − 2	3·386 − 2	3·047 − 2
12	13	4·920 − 2	4·353 − 2	3·869 − 2	3·456 − 2	2·808 − 2	2·343 − 2	2·008 − 2	1·765 − 2	1·590 − 2
12	14	9·902 − 2	8·829 − 2	7·890 − 2	7·068 − 2	5·722 − 2	4·697 − 2	3·913 − 2	3·314 − 2	2·861 − 2
12	15	1·454 − 1	1·436 − 1	1·430 − 1	1·426 − 1	1·428 − 1	1·441 − 1	1·459 − 1	1·479 − 1	1·501 − 1
13	14	9·036 − 3	8·805 − 3	8·724 − 3	8·762 − 3	9·085 − 3	9·590 − 3	1·015 − 2	1·069 − 2	1·118 − 2
13	15	9·797 − 2	8·798 − 2	7·928 − 2	7·168 − 2	5·914 − 2	4·926 − 2	4·126 − 2	3·470 − 2	2·945 − 2
14	15	2·227 − 2	1·949 − 2	1·718 − 2	1·524 − 2	1·229 − 2	1·019 − 2	8·617 − 3	7·360 − 3	6·298 − 3

Table 6. Comparison of our *LS R*-matrix results (a) and the relativistic distorted wave results of Zhang *et al* [18] (b) for transitions between the ground level $2p^6\ ^1S_0^e$ and the (nearly) pure $2p^5 3l\ ^{2S+1}L_J^\pi$ levels for selected energy ratios E/E_I, where E_I is the relevant exciation threshold energy. Our *LSJ* results are deduced from the *LS* results by an algebraic recoupling analogous to relation (9).

Transition		Calc.	Energy ratio E/E_I		
			1·2	1·5	1·9
$2b^6\,^1S_0^e$	$2p^5 3s\,^3P_2^0$	*a*		1·282 − 3	8·856 − 4
		b		0·904 − 3	6·90 − 4
	$2p^5 3d\,^3P_2^0$	*a*	8·044 − 3	5·672 − 3	3·916 − 3
		b	5·73 − 3	4·31 − 3	3·99 − 3
	$2p^5 3p\,^1S_0^e$	*a*	3·516 − 2	2·832 − 2	3·483 − 2
		b	3·90 − 2	4·03 − 2	4·16 − 3

the spin-allowed monopole transition $2p^6\,^1S_0^e - 2p^5 3p\,^1S_0^e$, the energy variations of the two calculations differ qualitatively, since the RDW results increase monotonically and slowly in this energy range, while the RM results present a minimum around $E/E_I = 1{\cdot}5$ and rise more sharply at high energies. These differences may be related to the fact that the RM calculation accounts non perturbatively and thoroughly for the strong monopole coupling.

Since the excitation collision strengths vary rapidly with energy in the threshold region, it is not practicable to tabulate them here. However, for many plasma applications, excitation rate coefficients rather than collision strengths are needed. They are obtained by integrating the collision strengths over the distribution of incident electron velocities. While Maxwellian distributions' are the usual distributions in astrophysical plasmas in local thermodynamical equilibrium, the effective collision rates for any other distribution could be calculated using our collision strengths listed in table 5. The excitation rate coefficient [19] for a transition from state i to state f at an electron temperature T is given by:

$$C(i \to f) = \frac{8{\cdot}6287 \times 10^{-6}}{g_i T^{1/2}} \gamma(i \to f) \exp\left[-\frac{\Delta E_{if}}{kT} \right] \text{cm}^3\,\text{s}^{-1}, \tag{7}$$

where $g_i = (2L_i + 1)(2S_i + 1)$ is the statistical weight of the lower state i, $\Delta E_{if} = E_f - E_i$ is the excitation energy and $\gamma(i \to f)$ is the effective collision strength defined as:

$$\gamma(i \to f) = \int_0^\infty \Omega(i \to f) \exp(-\varepsilon_f/\text{kT})\, d(\varepsilon_f/kT), \tag{8}$$

where $\Omega(i \to f)$ is the dimensionless collision strength for the transition from i to f, ε_f is the energy of the incident electron with respect to upper level f, and k is the Boltzmann constant. To perform the infinite integral in (8), the collision strengths were fitted to the correct asymptotic form as described by Berrington *et al* [19].

In table 7, we have given $\gamma(i \to f)$ for all the 105 transitions between the ground state and the $n = 3$ Rydberg states, over a wide range of electron temperatures, from $\log T = 5{\cdot}4$ to $\log T = 7{\cdot}0$, where T is given in °K. In general, the values of effective

Table 7. Effective collision strengths for transitions in Ni XIX. ($a \pm b \equiv a \times 10^{\pm b}$).

Transition		Temperature (log K)										
i	*f*	5·40	5·60	5·80	6·00	6·20	6·40	6·50	6·70	6·80	6·90	7·00
1	2	4·966 − 2	4·091 − 2	3·190 − 2	2·386 − 2	1·739 − 2	1·251 − 2	1·059 − 2	7·580 − 3	6·411 − 3	5·420 − 3	4·577 − 3
1	3	4·665 − 2	4·226 − 2	3·495 − 2	2·707 − 2	2·024 − 2	1·508 − 2	1·316 − 2	1·074 − 2	1·040 − 2	1·082 − 2	1·213 − 2
1	4	1·604 − 2	1·411 − 2	1·188 − 2	9·777 − 3	7·980 − 3	6·505 − 3	5·875 − 3	4·791 − 3	4·313 − 3	3·863 − 3	3·433 − 3
1	5	3·405 − 2	3·087 − 2	2·617 − 2	2·134 − 2	1·708 − 2	1·355 − 2	1·206 − 2	9·550 − 3	8·467 − 3	7·465 − 3	6·527 − 3
1	6	1·478 − 2	1·227 − 2	9·992 − 3	8·185 − 3	6·896 − 3	6·082 − 3	5·833 − 3	5·595 − 3	5·576 − 3	5·596 − 3	5·635 − 3
1	7	1·186 − 2	1·012 − 2	8·374 − 3	6·837 − 3	5·563 − 3	4·517 − 3	4·066 − 3	3·277 − 3	2·923 − 3	2·588 − 3	2·269 − 3
1	8	1·762 − 2	1·428 − 2	1·096 − 2	8·120 − 3	5·896 − 3	4·247 − 3	3·604 − 3	2·605 − 3	2·218 − 3	1·887 − 3	1·602 − 3
1	9	4·603 − 2	4·335 − 2	4·085 − 2	3·867 − 2	3·676 − 2	3·522 − 2	3·465 − 2	3·346 − 2	3·243 − 2	3·090 − 2	2·883 − 2
1	10	2·081 − 2	1·966 − 2	1·856 − 2	1·745 − 2	1·625 − 2	1·487 − 2	1·408 − 2	1·229 − 2	1·127 − 2	1·018 − 2	9·058 − 3
1	11	1·867 − 2	1·761 − 2	1·661 − 2	1·560 − 2	1·445 − 2	1·310 − 2	1·235 − 2	1·069 − 2	9·768 − 3	8·803 − 3	7·815 − 3
1	12	4·354 − 3	3·997 − 3	3·761 − 3	3·629 − 3	3·587 − 3	3·638 − 3	3·705 − 3	3·924 − 3	4·066 − 3	4·212 − 3	4·345 − 3
1	13	8·085 − 3	7·471 − 3	6·925 − 3	6·400 − 3	5·843 − 3	5·221 − 3	4·885 − 3	4·160 − 3	3·774 − 3	3·378 − 3	2·981 − 3
1	14	5·020 − 3	4·041 − 3	3·340 − 3	2·824 − 3	2·418 − 3	2·074 − 3	1·919 − 3	1·653 − 3	1·557 − 3	1·501 − 3	1·492 − 3
1	15	9·196 − 2	9·312 − 2	9·494 − 2	9·762 − 2	1·016 − 1	1·074 − 1	1·112 − 1	1·199 − 1	1·238 − 1	1·264 − 1	1·270 − 1
2	3	3·558 − 1	3·071 − 1	2·486 − 1	1·939 − 1	1·489 − 1	1·142 − 1	1·002 − 1	7·750 − 2	6·817 − 2	5·984 − 2	5·231 − 2
2	4	1·015 − 0	1·019 − 0	1·064 − 0	1·146 − 0	1·253 − 0	1·375 − 0	1·441 − 0	1·582 − 0	1·658 − 0	1·738 − 0	1·820 − 0
2	5	5·550 − 0	5·670 − 0	5·994 − 0	6·490 − 0	7·088 − 0	7·742 − 0	8·085 − 0	8·805 − 0	9·185 − 0	9·575 − 0	9·964 − 0
2	6	6·762 − 2	5·616 − 2	4·510 − 2	3·551 − 2	2·768 − 2	2·144 − 2	1·881 − 2	1·435 − 2	1·246 − 2	1·077 − 2	9·253 − 3
2	7	3·681 − 0	3·722 − 0	3·867 − 0	4·101 − 0	4·398 − 0	4·746 − 0	4·951 − 0	5·577 − 0	6·133 − 0	6·971 − 0	8·151 − 0
2	8	3·967 − 2	3·527 − 2	2·947 − 2	2·361 − 2	1·845 − 2	1·422 − 2	1·242 − 2	9·386 − 3	8·111 − 3	6·974 − 3	5·965 − 3
2	9	1·010 − 2	8·351 − 3	6·782 − 3	5·466 − 3	4·391 − 3	3·510 − 3	3·127 − 3	2·455 − 3	2·160 − 3	1·891 − 3	1·647 − 3
2	10	2·286 − 1	2·248 − 1	2·233 − 1	2·256 − 1	2·341 − 1	2·496 − 1	2·591 − 1	2·745 − 1	2·759 − 1	2·705 − 1	2·581 − 1
2	11	4·867 − 1	4·893 − 1	4·931 − 1	4·973 − 1	5·019 − 1	5·066 − 1	5·086 − 1	5·068 − 1	4·993 − 1	4·845 − 1	4·613 − 1
2	12	2·363 − 2	2·283 − 2	2·180 − 2	2·043 − 2	1·866 − 2	1·649 − 2	1·529 − 2	1·272 − 2	1·140 − 2	1·008 − 2	8·799 − 3
2	13	3·373 − 1	3·398 − 1	3·425 − 1	3·452 − 1	3·479 − 1	3·509 − 1	3·523 − 1	3·529 − 1	3·502 − 1	3·441 − 1	3·338 − 1
2	14	1·677 − 2	1·621 − 2	1·547 − 2	1·449 − 2	1·323 − 2	1·171 − 2	1·091 − 2	9·588 − 3	9·386 − 3	9·776 − 3	1·094 − 2
2	15	1·052 − 2	1·023 − 2	9·818 − 3	9·237 − 3	8·462 − 3	7·497 − 3	6·955 − 3	5·792 − 3	5·191 − 3	4·593 − 3	4·010 − 3

3	4	2·688 − 2	2·154 − 2	1·652 − 2	1·231 − 2	9·024 − 3	6·567 − 3	5·593 − 3	4·041 − 3	3·425 − 3	2·895 − 3	2·438 − 3
3	5	8·201 − 2	6·879 − 2	5·513 − 2	4·290 − 2	3·288 − 2	2·500 − 2	2·174 − 2	1·630 − 2	1·402 − 2	1·200 − 2	1·019 − 2
3	6	1·876 − 0	1·905 − 0	2·016 − 0	2·191 − 0	2·401 − 0	2·630 − 0	2·749 − 0	2·994 − 0	3·116 − 0	3·235 − 0	3·343 − 0
3	7	3·809 − 2	3·343 − 2	2·774 − 2	2·216 − 2	1·733 − 2	1·338 − 2	1·171 − 2	8·876 − 3	7·683 − 3	6·617 − 3	5·668 − 3
3	8	1·197 − 0	1·203 − 0	1·249 − 0	1·329 − 0	1·431 − 0	1·549 − 0	1·613 − 0	1·755 − 0	1·835 − 0	1·923 − 0	2·019 − 0
3	9	4·572 − 1	4·540 − 1	4·587 − 1	4·706 − 1	4·896 − 1	5·163 − 1	5·328 − 1	5·743 − 1	6·006 − 1	6·318 − 1	6·679 − 1
3	10	1·429 − 2	1·271 − 2	1·138 − 2	1·018 − 2	8·993 − 3	7·772 − 3	7·155 − 3	5·923 − 3	5·313 − 3	4·710 − 3	4·125 − 3
3	11	2·875 − 2	2·631 − 2	2·411 − 2	2·194 − 2	1·962 − 2	1·709 − 2	1·576 − 2	1·299 − 2	1·160 − 2	1·022 − 2	8·891 − 3
3	12	1·455 − 1	1·477 − 1	1·500 − 1	1·524 − 1	1·550 − 1	1·579 − 1	1·595 − 1	1·631 − 1	1·651 − 1	1·672 − 1	1·694 − 1
3	13	1·603 − 2	1·549 − 2	1·480 − 2	1·388 − 2	1·271 − 2	1·129 − 2	1·049 − 2	8·783 − 3	7·889 − 3	6·993 − 3	6·115 − 3
3	14	1·063 − 1	1·060 − 1	1·060 − 1	1·063 − 1	1·071 − 1	1·084 − 1	1·091 − 1	1·102 − 1	1·100 − 1	1·091 − 1	1·070 − 1
3	15	6·783 − 2	6·822 − 2	6·886 − 2	6·975 − 2	7·090 − 2	7·236 − 2	7·313 − 2	7·385 − 2	7·313 − 2	7·121 − 2	6·795 − 2
4	5	2·826 − 1	2·606 − 1	2·391 − 1	2·200 − 1	2·038 − 1	1·906 − 1	1·863 − 1	1·904 − 1	2·042 − 1	2·290 − 1	2·649 − 1
4	6	4·033 − 2	3·311 − 2	2·618 − 2	2·036 − 2	1·582 − 2	1·238 − 2	1·099 − 2	8·685 − 3	7·704 − 3	6·800 − 3	5·956 − 3
4	7	2·639 − 1	2·153 − 1	1·650 − 1	1·216 − 1	8·794 − 2	6·385 − 2	5·649 − 2	6·403 − 2	8·949 − 2	1·375 − 1	2·115 − 1
4	8	2·172 − 2	1·735 − 2	1·322 − 2	9·837 − 3	7·277 − 3	5·407 − 3	4·675 − 3	3·509 − 3	3·036 − 3	2·618 − 3	2·245 − 3
4	9	7·945 − 3	7·066 − 3	6·308 − 3	5·650 − 3	5·056 − 3	4·519 − 3	4·326 − 3	4·649 − 3	5·625 − 3	7·503 − 3	1·044 − 2
4	10	1·620 − 0	1·703 − 0	1·792 − 0	1·890 − 0	1·999 − 0	2·122 − 0	2·192 − 0	2·346 − 0	2·431 − 0	2·519 − 0	2·609 − 0
4	11	3·384 − 2	3·344 − 2	3·296 − 2	3·239 − 2	3·173 − 2	3·108 − 2	3·078 − 2	3·009 − 2	2·951 − 2	2·861 − 2	2·731 − 2
4	12	9·163 − 3	8·856 − 3	8·434 − 3	7·867 − 3	7·140 − 3	6·266 − 3	5·788 − 3	4·785 − 3	4·276 − 3	3·775 − 3	3·290 − 3
4	13	7·582 − 3	7·250 − 3	6·820 − 3	6·276 − 3	5·621 − 3	4·869 − 3	4·470 − 3	3·679 − 3	3·314 − 3	2·984 − 3	2·696 − 3
4	14	2·746 − 3	2·583 − 3	2·387 − 3	2·153 − 3	1·878 − 3	1·574 − 3	1·424 − 3	1·200 − 3	1·177 − 3	1·261 − 3	1·480 − 3
4	15	7·709 − 3	7·468 − 3	7·127 − 3	6·655 − 3	6·042 − 3	5·304 − 3	4·901 − 3	4·060 − 3	3·632 − 3	3·210 − 3	2·801 − 3
5	6	2·265 − 1	1·940 − 1	1·618 − 1	1·332 − 1	1·094 − 1	8·991 − 2	8·172 − 2	6·902 − 2	6·496 − 2	6·268 − 2	6·213 − 2
5	7	1·633 − 0	1·505 − 0	1·347 − 0	1·192 − 0	1·061 − 0	9·604 − 1	9·270 − 1	9·428 − 1	1·031 − 0	1·202 − 0	1·469 − 0
5	8	1·614 − 1	1·454 − 1	1·256 − 1	1·059 − 1	8·843 − 2	7·340 − 2	6·682 − 2	5·577 − 2	5·145 − 2	4·794 − 2	4·518 − 2
5	9	2·127 − 2	1·776 − 2	1·473 − 2	1·227 − 2	1·032 − 2	8·745 − 3	8·051 − 3	6·747 − 3	6·105 − 3	5·461 − 3	4·822 − 3
5	10	1·343 − 1	1·214 − 1	1·122 − 1	1·058 − 1	1·014 − 1	9·884 − 2	9·835 − 2	9·974 − 2	1·020 − 1	1·054 − 1	1·097 − 1
5	11	6·830 − 0	7·357 − 0	7·886 − 0	8·412 − 0	8·954 − 0	9·528 − 0	9·804 − 0	1·012 + 01	1·004 + 01	9·733 − 0	9·205 − 0
5	12	5·152 − 2	4·954 − 2	4·701 − 2	4·374 − 2	3·964 − 2	3·478 − 2	3·214 − 2	2·657 − 2	2·374 − 2	2·094 − 2	1·823 − 2
5	13	1·507 − 0	1·556 − 0	1·609 − 0	1·670 − 0	1·742 − 0	1·832 − 0	1·885 − 0	2·006 − 0	2·074 − 0	2·146 − 0	2·218 − 0
5	14	2·754 − 2	2·647 − 2	2·507 − 2	2·327 − 2	2·101 − 2	1·835 − 2	1·692 − 2	1·394 − 2	1·245 − 2	1·098 − 2	9·577 − 3
5	15	1·699 − 2	1·645 − 2	1·568 − 2	1·460 − 2	1·319 − 2	1·149 − 2	1·058 − 2	8·704 − 3	7·766 − 3	6·846 − 3	5·961 − 3

(Continued)

Table 7. (*Continued*)

Transition		Temperature (log K)										
i	*f*	5·40	5·60	5·80	6·00	6·20	6·40	6·50	6·70	6·80	6·90	7·00
6	7	1·704 − 1	1·514 − 1	1·296 − 1	1·086 − 1	9·011 − 2	7·438 − 2	6·760 − 2	5·707 − 2	5·403 − 2	5·301 − 2	5·420 − 2
6	8	5·065 − 1	4·595 − 1	4·081 − 1	3·614 − 1	3·236 − 1	2·951 − 1	2·837 − 1	2·639 − 1	2·534 − 1	2·410 − 1	2·258 − 1
6	9	5·190 − 2	4·932 − 2	4·730 − 2	4·579 − 2	4·469 − 2	4·387 − 2	4·344 − 2	4·182 − 2	4·025 − 2	3·804 − 2	3·520 − 2
6	10	3·176 − 2	2·631 − 2	2·212 − 2	1·879 − 2	1·595 − 2	1·337 − 2	1·214 − 2	9·778 − 3	8·654 − 3	7·579 − 3	6·564 − 3
6	11	6·930 − 2	6·094 − 2	5·420 − 2	4·815 − 2	4·220 − 2	3·608 − 2	3·297 − 2	2·677 − 2	2·373 − 2	2·080 − 2	1·801 − 2
6	12	2·328 − 0	2·492 − 0	2·655 − 0	2·819 − 0	2·994 − 0	3·187 − 0	3·294 − 0	3·527 − 0	3·652 − 0	3·778 − 0	3·898 − 0
6	13	2·699 − 2	2·608 − 2	2·482 − 2	2·312 − 2	2·094 − 2	1·833 − 2	1·691 − 2	1·394 − 2	1·244 − 2	1·097 − 2	9·559 − 3
6	14	4·883 − 1	5·064 − 1	5·265 − 1	5·493 − 1	5·767 − 1	6·100 − 1	6·289 − 1	6·688 − 1	6·871 − 1	7·014 − 1	7·094 − 1
6	15	1·567 − 2	1·577 − 2	1·595 − 2	1·622 − 2	1·664 − 2	1·727 − 2	1·767 − 2	1·872 − 2	1·940 − 2	2·022 − 2	2·117 − 2
7	8	2·674 − 1	2·280 − 1	1·818 − 1	1·384 − 1	1·027 − 1	7·552 − 2	6·490 − 2	4·920 − 2	4·419 − 2	4·119 − 2	4·017 − 2
7	9	4·893 − 3	4·228 − 3	3·655 − 3	3·181 − 3	2·783 − 3	2·431 − 3	2·263 − 3	1·928 − 3	1·754 − 3	1·577 − 3	1·397 − 3
7	10	1·288 − 0	1·361 − 0	1·442 − 0	1·528 − 0	1·622 − 0	1·728 − 0	1·787 − 0	1·918 − 0	1·989 − 0	2·061 − 0	2·130 − 0
7	11	1·224 − 1	1·090 − 1	9·891 − 2	9·115 − 2	8·491 − 2	7·990 − 2	7·807 − 2	7·714 − 2	7·885 − 2	8·238 − 2	8·765 − 2
7	12	2·106 − 2	1·989 − 2	1·865 − 2	1·719 − 2	1·545 − 2	1·346 − 2	1·238 − 2	1·017 − 2	9·066 − 3	7·981 − 3	6·939 − 3
7	13	4·115 − 0	4·326 − 0	4·546 − 0	4·777 − 0	5·031 − 0	5·322 − 0	5·485 − 0	5·837 − 0	6·014 − 0	6·181 − 0	6·322 − 0
7	14	2·782 − 2	2·690 − 2	2·562 − 2	2·390 − 2	2·166 − 2	1·898 − 2	1·752 − 2	1·447 − 2	1·294 − 2	1·144 − 2	9·984 − 3
7	15	9·355 − 3	9·042 − 3	8·596 − 3	7·982 − 3	7·190 − 3	6·251 − 3	5·746 − 3	4·708 − 3	4·189 − 3	3·682 − 3	3·196 − 3
8	9	3·014 − 1	2·080 − 1	1·402 − 1	9·287 − 2	6·085 − 2	3·962 − 2	3·193 − 2	2·073 − 2	1·669 − 2	1·343 − 2	1·080 − 2
8	10	1·450 − 2	1·243 − 2	1·070 − 2	9·232 − 3	7·905 − 3	6·652 − 3	6·043 − 3	4·861 − 3	4·295 − 3	3·754 − 3	3·245 − 3
8	11	3·341 − 2	2·861 − 2	2·461 − 2	2·120 − 2	1·816 − 2	1·531 − 2	1·392 − 2	1·124 − 2	9·947 − 3	8·702 − 3	7·524 − 3
8	12	1·659 − 2	1·595 − 2	1·559 − 2	1·546 − 2	1·554 − 2	1·583 − 2	1·606 − 2	1·665 − 2	1·697 − 2	1·725 − 2	1·747 − 2
8	13	2·926 − 2	2·785 − 2	2·620 − 2	2·423 − 2	2·187 − 2	1·915 − 2	1·767 − 2	1·459 − 2	1·302 − 2	1·147 − 2	9·983 − 3
8	14	1·357 − 0	1·425 − 0	1·498 − 0	1·575 − 0	1·662 − 0	1·763 − 0	1·823 − 0	2·005 − 0	2·157 − 0	2·375 − 0	2·670 − 0
8	15	4·920 − 1	4·979 − 1	5·067 − 1	5·197 − 1	5·388 − 1	5·654 − 1	5·814 − 1	6·137 − 1	6·248 − 1	6·278 − 1	6·194 − 1

9	10	1·026 − 2	9·413 − 3	8·564 − 3	7·696 − 3	6·777 − 3	5·808 − 3	5·315 − 3	4·337 − 3	3·859 − 3	3·394 − 3	2·950 − 3
9	11	1·594 − 2	1·391 − 2	1·204 − 2	1·036 − 2	8·813 − 3	7·359 − 3	6·667 − 3	5·355 − 3	4·736 − 3	4·146 − 3	3·590 − 3
9	12	6·437 − 3	6·329 − 3	6·298 − 3	6·361 − 3	6·531 − 3	6·821 − 3	7·011 − 3	7·473 − 3	7·738 − 3	8·015 − 3	8·293 − 3
9	13	3·709 − 3	3·311 − 3	2·931 − 3	2·565 − 3	2·199 − 3	1·833 − 3	1·654 − 3	1·310 − 3	1·149 − 3	9·978 − 4	8·569 − 4
9	14	5·758 − 3	4·516 − 3	3·445 − 3	2·604 − 3	1·966 − 3	1·487 − 3	1·294 − 3	9·990 − 4	9·073 − 4	8·654 − 4	8·814 − 4
9	15	6·058 − 1	6·154 − 1	6·311 − 1	6·534 − 1	6·829 − 1	7·200 − 1	7·427 − 1	8·080 − 1	8·610 − 1	9·367 − 1	1·040 − 0
10	11	2·145 − 1	2·046 − 1	1·942 − 1	1·825 − 1	1·694 − 1	1·637 − 1	1·855 − 1	4·650 − 1	8·727 − 1	1·580 − 0	2·648 − 0
10	12	7·116 − 2	6·893 − 2	6·591 − 2	6·192 − 2	5·685 − 2	5·081 − 2	4·755 − 2	4·109 − 2	3·816 − 2	3·557 − 2	3·336 − 2
10	13	2·897 − 1	2·862 − 1	2·803 − 1	2·714 − 1	2·594 − 1	2·455 − 1	2·388 − 1	2·298 − 1	2·288 − 1	2·303 − 1	2·339 − 1
10	14	3·335 − 2	3·212 − 2	3·046 − 2	2·832 − 2	2·567 − 2	2·264 − 2	2·105 − 2	1·787 − 2	1·631 − 2	1·474 − 2	1·317 − 2
10	15	3·613 − 2	3·500 − 2	3·343 − 2	3·136 − 2	2·877 − 2	2·576 − 2	2·418 − 2	2·130 − 2	2·025 − 2	1·961 − 2	1·943 − 2
11	12	2·043 − 1	1·978 − 1	1·889 − 1	1·771 − 1	1·624 − 1	1·448 − 1	1·353 − 1	1·168 − 1	1·087 − 1	1·019 − 1	9·673 − 2
11	13	6·518 − 1	6·457 − 1	6·365 − 1	6·237 − 1	6·081 − 1	5·906 − 1	5·824 − 1	5·743 − 1	5·783 − 1	5·894 − 1	6·073 − 1
11	14	1·437 − 1	1·393 − 1	1·333 − 1	1·253 − 1	1·151 − 1	1·027 − 1	9·592 − 2	8·179 − 2	7·485 − 2	6·829 − 2	6·227 − 2
11	15	6·939 − 2	6·743 − 2	6·465 − 2	6·085 − 2	5·596 − 2	5·005 − 2	4·679 − 2	3·989 − 2	3·634 − 2	3·279 − 2	2·927 − 2
12	13	1·430 − 1	1·390 − 1	1·334 − 1	1·256 − 1	1·156 − 1	1·034 − 1	9·660 − 2	8·219 − 2	7·491 − 2	6·781 − 2	6·103 − 2
12	14	1·477 − 1	1·481 − 1	1·481 − 1	1·477 − 1	1·469 − 1	1·462 − 1	1·459 − 1	1·452 − 1	1·442 − 1	1·423 − 1	1·390 − 1
12	15	1·011 − 2	9·976 − 3	9·811 − 3	9·624 − 3	9·450 − 3	9·371 − 3	9·406 − 3	9·745 − 3	1·010 − 2	1·060 − 2	1·122 − 2
13	14	1·417 − 1	1·377 − 1	1·320 − 1	1·243 − 1	1·146 − 1	1·028 − 1	9·624 − 2	8·193 − 2	7·433 − 2	6·658 − 2	5·883 − 2
13	15	3·357 − 2	3·244 − 2	3·087 − 2	2·879 − 2	2·621 − 2	2·318 − 2	2·155 − 2	1·817 − 2	1·648 − 2	1·483 − 2	1·323 − 2
14	15	5·855 − 2	5·823 − 2	5·784 − 2	5·732 − 2	5·668 − 2	5·600 − 2	5·567 − 2	5·507 − 2	5·482 − 2	5·461 − 2	5·439 − 2

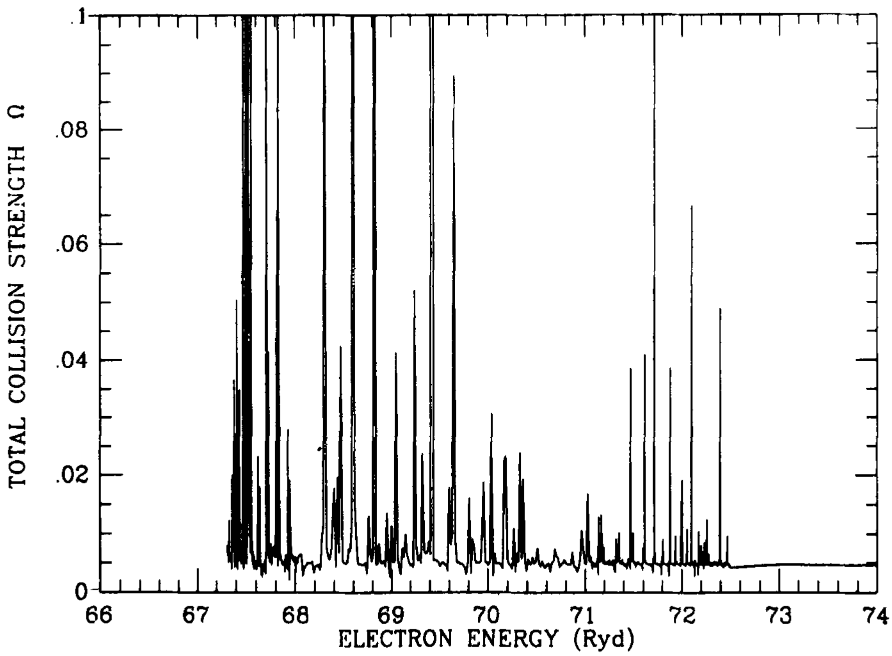

Figure 2. Total collision strength for the transition $1s^2 2s^2 2p^6\,{}^1S^e \rightarrow 1s^2 2s^2 2p^5 3s\,{}^1P^0$ in Ni XIX as a function of electron energy in Rydberg.

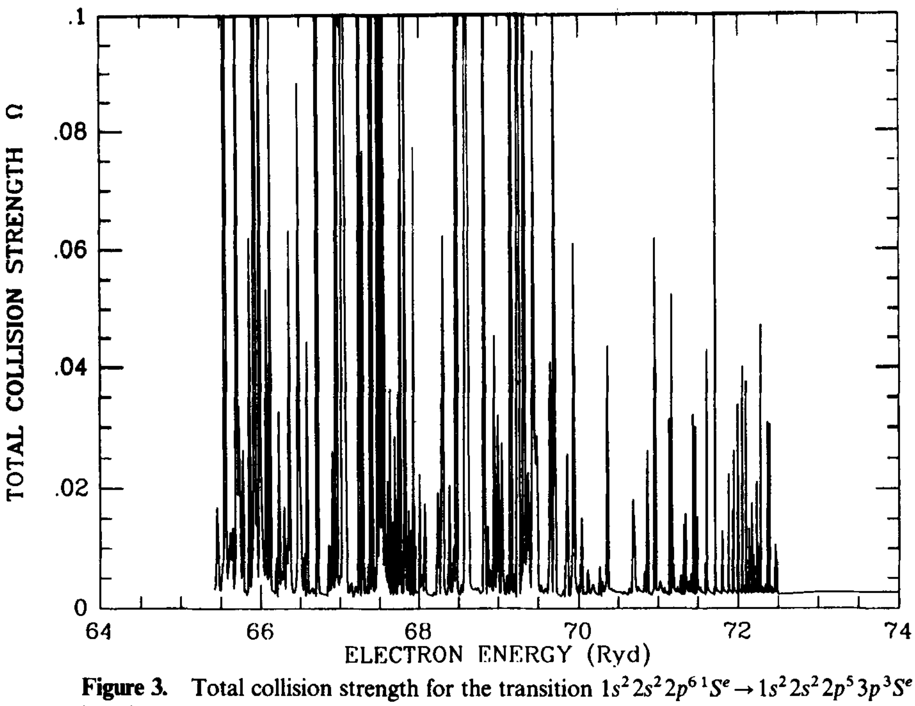

Figure 3. Total collision strength for the transition $1s^2 2s^2 2p^6\,{}^1S^e \rightarrow 1s^2 2s^2 2p^5 3p\,{}^3S^e$ in Ni XIX as a function of electron energy in Rydberg.

collision strengths γ are larger for allowed transitions than for spin-forbidden transitions. Among the $2p^6\,{}^1S^e \rightarrow 2p^5\,3p$ transitions, the value of γ is largest for the monopole-allowed $2p^6\,{}^1S^e$–$2p^5\,3p\,{}^1S^e$ transition, as already found by Zhang *et al* [18, 20]. In contrast, for the $2p^6\,{}^1S^e - 2p^5\,3d$ transitions, the largest γ corresponds to the dipole-allowed $2p^6\,{}^1S^e - 2p^5\,3d\,{}^1P^0$ transition, which involves the promotion of a $2p$ electron to a $3d$ orbital. Similarly, for the transitions from $2p^5\,3s\,{}^3P^0$, the largest γ corresponds to the dipole-allowed $2p^5\,3s\,{}^3P^0 - 2p^5\,3d\,{}^2D^e$ transition. Among all the 105 transitions, the value of γ is the largest for the $2p^5\,3p\,{}^3D^e \rightarrow 2p^5\,3d\,{}^3F^0$ transition, which is again dipole-allowed and involves the promotion of a $3p$ electron to a $3d$ orbital. The next largest γ corresponds to the $2p^5\,3p\,{}^3P^e \rightarrow 2p^5\,3d\,{}^3D^0$ transition.

Since the ground state $2p^6\,{}^1S^e$ and the singlet excited states $2p^5\,3s\,{}^1P^0$, $2p^5\,3p\,{}^1D^e$, ${}^1P^e$, ${}^1S^e$ and $2p^5\,3d\,{}^1F^0$, ${}^1D^0$, ${}^1P^0$ states have no fine structure, if one assumes the term mixing to be negligible, one can easily deduce the effective collision strengths for the transitions between their fine structure sublevels, from our results in the *LS* coupling scheme using the following relation:

$$\frac{1}{2J+1}\gamma({}^1L_L^{\pi} - {}^3L_J'^{\pi'}) = \frac{1}{3(2L'+1)}\gamma({}^1L^{\pi} - {}^3L'^{\pi'}). \tag{9}$$

5. Conclusion

The conclude, we would like to mention that, to date, our results are the only collision strengths and rate coefficients available for all the 105 transitions between the ground and the $n = 3$ Rydberg states of Ni XIX, where the influence of resonance effects is included. We have accounted for exchange, channel coupling, short range correlation effects and the contribution of higher partial waves. On the other hand, we have made no allowance for relativistic effects, either in the target wave-functions or in the scattering calculations.

Acknowledgements

We would like to thank the Indo-French Centre for the Promotion of Advanced Research/Centre Franco-Indien pour la Promotion de la Recherche Avancée and the EC contract SCI-0168C for financial support. One of us (MM) is thankful to DST (India), UGC (India) and SERC (UK) for financial support. (MM an IUCAA associate) is also thankful to Inter University Centre for Astronomy and Astrophysics (IUCAA) for facilities and financial support. The computing in this work was carried out on the CRAY-XMP/48 at the Rutherford Appleton Laboratory, UK, via a workstation at the Queen's University of Belfast. The allocation of computer time under a SERC Rolling Grant is gratefully acknowledged.

References

[1] R K Janev, *Phys. Scr.* **T37**, 5–7 (1991)
[2] D L Matthews, *et al*, *Phys. Rev. Lett.* **54**, 110–113 (1985)
[3] U Feldman, L Cohen and M Swartz, *Astrophys. J.* **148**, 585 (1967)
[4] M Swartz, S Kastner, E Rothe and W Neupert *J. Phys.* **4**, 1747 (1971)
[5] A K Bhatia, U Feldman and J F Seely, *At. Data Nucl. Data Tables* **32**, 435–467 (1985)
[6] P L Hagelstein and R K Jung, *At. Data Nucl. Data Tables* **37**, 64–121 (1987)
[7] P G Burke and W D Robb, *Adv. At. Mol. Phys.* **11**, 143–214 (1975)

[8] K A Berrington, P G Burke, M Le Dourneuf, W D Robb, K T Taylor and L Vo Ky, *Comput. Phys. Commun.* **14**, 367 (1978)
[9] K A Berrington, P G Burke, K Butler, M J Seaton, P J Storey, K T Taylor and Y Yu, *J. Phys.* **B20**, 6379 (1987)
[10] V M Burke, P G Burke and N S Scott, *Comput. Phys. Commun.*, in press (1991)
[11] A Burgess, D G Hummer and J A Tully, *Proc. Trans. R. Soc.* **A266**, 225 (1970)
[12] A Hibbert, *Comput. Phys. Commun.* **9**, 141–172 (1975)
[13] A Hibbert, M Le Dourneuf and M Mohan (to be published) (1991)
[14] E Clementi and C Roetti, *At. Data Nucl. Data Tables* **14**, 177–478 (1974)
[15] C Corliss and J Sugar, *J. Phys. Chem. Ref. Data* **10**, 278 (1981)
[16] P G Burke, K A Berrington and C V Sukumar, *J. Phys.* **B14**, 287 (1981)
[17] M J Seaton, *J. Phys.* **B18**, 2111–31 (1985)
[18] H Zhang and D H Sampson, *At. Data Nucl. Data Tables* **43**, 1–69 (1989)
[19] W Eissner and M J Seaton, *J. Phys.* **B7**, 2533–2548 (1974)
[20] H Zhang, D H Sampson, R E M Clark and J B Mann, *At. Data Nucl. Data Tables* **37**, 17–40 (1987)